



**HAL**  
open science

## **Iliac auricular surface morphofunctional study in felidae.**

Jean-Pierre Pallandre, Raphael Cornette, Marie-Ange Placide, Eric Pellé,  
Franck Lavenne, Vincent Abad, Mélina Ribaud, Vincent Bels

### ► To cite this version:

Jean-Pierre Pallandre, Raphael Cornette, Marie-Ange Placide, Eric Pellé, Franck Lavenne, et al.. Iliac auricular surface morphofunctional study in felidae.. *Zoology (Jena, Germany)*, 2020, 138, pp.125714. 10.1016/j.zool.2019.125714 . hal-02613166

**HAL Id: hal-02613166**

**<https://hal.science/hal-02613166>**

Submitted on 21 Jul 2022

**HAL** is a multi-disciplinary open access archive for the deposit and dissemination of scientific research documents, whether they are published or not. The documents may come from teaching and research institutions in France or abroad, or from public or private research centers.

L'archive ouverte pluridisciplinaire **HAL**, est destinée au dépôt et à la diffusion de documents scientifiques de niveau recherche, publiés ou non, émanant des établissements d'enseignement et de recherche français ou étrangers, des laboratoires publics ou privés.



Distributed under a Creative Commons Attribution - NonCommercial 4.0 International License

# 1 ILIAC AURICULAR SURFACE MORPHOFUNCTIONAL STUDY IN 2 FELIDAE

3  
4  
5 Jean-Pierre Pallandre<sup>1</sup>, Raphaël Cornette<sup>1</sup>, Marie-Ange Placide<sup>1</sup>, Eric Pelle<sup>2</sup>, Franck  
6 Lavenne<sup>3</sup>, Vincent Abad<sup>4</sup>, Mélina Ribaud<sup>5</sup>, and Vincent L. Bels<sup>1</sup>  
7  
8  
9  
10  
11

12 <sup>1</sup> Sorbonne Université, Muséum national d'Histoire naturelle, Institut de Systématique  
13 Evolution Biodiversité (UMR 7205 MNHN/CNRNS/UPMC/EPHE), 57 Rue Cuvier,  
14 75005 - Paris, France.

15 <sup>2</sup> Sorbonne Université, Muséum national d'Histoire naturelle, Direction Générale des  
16 collections, 57 Rue Cuvier, 75005 - Paris, France.

17 <sup>3</sup> Centre d'Etude et de Recherche Multimodale Et Pluridisciplinaire en imagerie du  
18 vivant (CNRS, INSB), 16-18 avenue Doyen Lépine, 69500 Bron, France.

19 <sup>4</sup> R & D, Manufacture des pneumatiques Michelin, 23 place des Carmes Dechaux,  
20 63040 Clermont-Ferrand, France.

21 <sup>5</sup> Université Lyon, Ecole Centrale de Lyon, Institut Camille Jordan, 36 avenue Guy de  
22 Collonge, 69134 Ecully, France.  
23  
24  
25  
26  
27  
28  
29  
30  
31

## 32 **Corresponding author:**

33 Dr Jean-Pierre Pallandre, Sorbonne Université, Muséum national d'Histoire naturelle,  
34 Institut de Systématique Evolution Biodiversité (UMR 7205  
35 MNHN/CNRNS/UPMC/EPHE), Paris – France. E-mail :  
36 jeanpierre.pallandre@wanadoo.fr

## 37 **Abstract**

38 Felids show remarkable phenotypic similarities and are conservative in behavioral  
39 and ecological traits. In contrast, they display a large range in body mass from  
40 around 1 kg to more than 300 kg. Body size and locomotory specializations correlate  
41 to skull, limb and vertebral skeleton morphology. With an increase in body mass,  
42 felids prey selection switches from small to large, from using a rapid skull or spine  
43 lethal bite for small prey, to sustained suffocating bite for large prey. Dietary  
44 specialization correlates to skull and front limbs morphology but no correlation was  
45 found on the spine or on the hind limb. The morphology of the sacroiliac junction in  
46 relation to ecological factors remained to be described. We are presenting a study of  
47 the overall shape of the iliac auricular surface with qualitative and quantitative  
48 analyses of its morphology. Our results demonstrate that body mass, prey selection,  
49 and bite type, crucially influence the auricular surface, where no significant effect of  
50 locomotor specialization was found. The outline of the surface is significantly more  
51 elevated dorso-caudally and the joint surface shows an irregular W-shape  
52 topography in big cats whereas the surface in small cats is smoother with a C-shape  
53 topography and less of an elevated ridge. Biomechanically, we suggest that a  
54 complex auricular surface increases joint stiffness and provides more support in  
55 heavier cats, an advantage for subduing big prey successfully during a sustained  
56 bite.

57

58 **Key words:** Felidae, ilium, evolution, pelvis, sacroiliac junction, auricular surface,  
59 predatory behavior, locomotion.

60

## 61 **1. Introduction**

62 All felids exhibit relatively little variation of body shape and lifestyle across their  
63 worldwide distribution (Martin, 1989; Rothwell, 2003; MacDonald, 2009; Sunquist and  
64 Sunquist, 2017; Piras et al., 2018). Regardless of their overall phenotypic similarities,  
65 they show an incredible range of size and mass from around 1 kg (*Prionailurus*  
66 *rubiginosus*) (Mattern and McLennan, 2000) to over 300 kg for *Panthera tigris*  
67 (Hayward et al., 2012). Cuff et al. (2015) demonstrated that felids show two selective  
68 body mass optima: (i) around 5 kg for “small cats”, and (ii) around 100 kg for “big  
69 cats”, and that their body masses were significantly different among prey choice

70 classes (small, mixed, large). Despite this variability in body mass, felids show a  
71 remarkable uniformity of limb posture compared to other mammals where increased  
72 body size generally leads to joint extension, reducing functional stress on supportive  
73 tissues (Biewener, 1989; Bertram and Biewener, 1990; Biewener and Patek, 2018).  
74 Instead, cross sections of long bones in felids follow an allometric relationship (Day  
75 and Jayne, 2007; Zhang et al., 2012).

76 For these carnivores a large number of functional studies, including paleontological  
77 investigations, suggest that locomotion and predatory behavior are major  
78 evolutionary pressures on body size and mass (Mattern and McLennan, 2000;  
79 Hayward and Kerley, 2005; Meachen-Samuels and Van Valkenburgh, 2009a, 2009b;  
80 Slater and Van Valkenburgh, 2009; Hayward et al., 2012; Samuels et al., 2013).  
81 Indeed, felids also show similarities in their behavior related to locomotion. They are  
82 able to forage in various habitats by using all different gaits and can also swim  
83 (Samuels et al., 2013). Unlike other carnivorans such as canids, front paws retractile  
84 claws and rotation of the elbow are features that make them excellent climbers  
85 (Gonyea, 1978; Andersson and Werdelin, 2003 ; Andersson, 2004). Some of them  
86 (e.g. *Neofelis nebulosa*) can even hunt in trees. Several authors classified felid  
87 locomotor behavior in three classes: (i) terrestrial for species that rarely swim or  
88 climb, (ii) scansorial for species able to climb but not to forage in trees, and (iii)  
89 arboreal for species actively foraging in trees (Meachen-Samuels and Van  
90 Valkenburgh, 2009a; Randau et al., 2016). But other authors determined that the  
91 cheetah (*Acinonyx jubatus*), which regularly displays rapid locomotion, should be  
92 classified as a (iiii) cursorial felid (Samuels et al., 2013; Martín-Serra et al., 2014).

93 Recent studies determined that the morphology of postcranial skeleton displayed  
94 differences among locomotor groups in the order of Carnivora (Samuels et al., 2013;  
95 Morales and Giannini, 2013, 2014 ; Martín-Serra et al., 2014; Cuff et al., 2015;  
96 Randau et al., 2016, 2017). Morphological indices of the limbs effectively distinguish  
97 locomotor groups among Carnivora, with cursorial and arboreal species more  
98 accurately classified than terrestrial, scansorial or semi-aquatic species (Samuels et  
99 al., 2013). Cursorial species exhibit distal lengthening of limbs and they have slender  
100 limbs elements and relatively narrow humeral and femoral epicondyles. Arboreal  
101 species show an elongation of manual digits and better hip abduction abilities  
102 whereas scansorial and terrestrial species display intermediate features (Samuels et  
103 al., 2013; Morales and Giannini, 2013, 2014 ; Morales et al., 2018). However, Martín-

104 Serra et al. (2014) demonstrated that different modes of locomotion had very little  
105 influence on the hind limb of carnivorans, compared to phylogeny and body size.  
106 Further investigations into the morphology of the vertebral column showed a  
107 significant difference in terrestrial, scansorial and arboreal felids, in the lumbar region  
108 more specifically, while dietary specialization did not influence the spine morphology  
109 (Randau et al., 2016, 2017). In contrast, studies have shown that limb morphology  
110 was indicative of hunting strategy and prey size specialization within Felidae in  
111 relation with prey manipulation during grabbing and subduing (Gonyea and  
112 Ashworth, 1975; Meachen-Samuels and Van Valkenburgh, 2009a; Meachen-  
113 Samuels, 2010; Janis and Figueirido, 2014; Cuff et al., 2016).

114 Predation in felids is a complex behavior involving optimization of quality and quantity  
115 of nutrients and energy intake (Leyhausen and Tonkin, 1979; Seidensticker and  
116 McDougal, 1993; Schaller, 2009; Tirok et al., 2011; Gittleman, 2013). Felids show  
117 various hunting behaviors (e.g. ambush, pursuit) to capture a large range of prey in  
118 various habitats (e.g. mountain, forest, savannah). This behavioral diversity reported  
119 between and within species (Caro and Fitzgibbon, 1992; Carbone et al., 2007; Kohl  
120 et al., 2015; Machovsky-Capuska et al., 2016) largely depends on environmental  
121 factors (Leyhausen and Tonkin, 1979; Gittleman, 2013). But prey preference is a key  
122 feature in felids behavior and morphology (Dickman, 1988; Labisky and Boulay,  
123 1998; Carbone et al., 1999, 2007; Meachen-Samuels and Van Valkenburgh, 2009a,  
124 2009b; Clements et al., 2014; Cuff et al., 2015). Meta-analyses demonstrate  
125 relationships between terrestrial predator mass (and size), prey diversity, and prey  
126 mass (and size). Small felids (e.g., Domestic cat lineage species) generally predate  
127 on a large amount of prey smaller and lighter than themselves (Dickman, 1988;  
128 Carbone et al., 2007). In comparison, large felids (e.g., *Panthera* lineage species)  
129 select bigger prey to sustain their increased physiological demands. Carbone et al.  
130 (1999, 2007) suggest that, reaching a threshold between 14.5 to 25 kg, predators  
131 start killing prey around 45% of their own body mass. Several authors classified  
132 relative prey size preference as: (i) small (selected prey is smaller than predator), (ii)  
133 large (prey is predator's own size or larger), and (iii) mixed prey (when both sizes of  
134 prey are selected depending on their availability and on individual preference)  
135 (Carbone et al., 2007; Meachen-Samuels and Van Valkenburgh, 2009a, 2009b; Cuff  
136 et al., 2015; Randau et al., 2016). Other authors use other criteria for prey selection  
137 such as the ratio between the maximum average prey mass (MPM) and the average

138 predator body mass (PBM) (Sicuro and Oliveira, 2011). Varying from 0.3 (*Catopuma*  
139 *badia* and *Pardofelis marmorata*) to 2.7 (*Panthera tigris*), this MPM/PBM ratio  
140 probably provides a better indicator for predators ability to select and kill big prey  
141 (Carbone et al., 2007; Sicuro and Oliveira, 2011). Indeed, within the *Panthera*  
142 lineage, all species are able to select prey with a ratio above 1.7. However, the  
143 clouded leopard (*Neofelis nebulosa*), being the smallest representative species of the  
144 *Panthera* lineage (19.5 kg), shows a MPM/PBM ratio of 2.7. This ratio is similar to  
145 that of the largest *Panthera tigris* with an average body weight around 185.0 kg,  
146 which questions the correlation between body mass and big prey selection abilities.

147 Preying on very large prey is a real challenge for felids, which are known to be  
148 solitary, stalking predators (Leyhausen and Tonkin, 1979; Gittleman, 2013). To  
149 increase their chance for energy intake (Sunquist and Sunquist, 1989; Kleiman and  
150 Eisenberg, 1973; Rudnai, 2012; Bailey et al., 2013) and to decrease the risk of  
151 struggling with large dangerous prey (MacNulty et al., 2007; Mukherjee and Heithaus,  
152 2013), some individuals occasionally cooperate for hunting sessions. For example,  
153 little groups of cheetahs are known to form stable hunting coalitions (Caro, 1994;  
154 Radloff and Du Toit, 2004). However, lions (*Panthera leo*) are the only species to  
155 have a regular social life within Felidae (Pulliam and Caraco, 1984; Scheel and  
156 Packer, 1991; Stander, 1992; Schaller, 2009). Pack life in open habitats with an  
157 ambush hunting style leads to pack hunting strategies (Kitchener et al., 2010;  
158 Davidson et al., 2013).

159 Feeding constraints are typically associated with the cranial system (e.g., jaw  
160 morphology, tooth shape). Indeed the jaw apparatus, which determines the bite  
161 force, plays the key role in killing any kind of prey (Leyhausen and Tonkin, 1979).  
162 The strength of this apparatus is sufficient to kill small prey. In contrast, to kill large  
163 and heavy prey that struggles, felids have to cope with other functional constraints.  
164 Felid species are known to have different killing strategies in relation to prey size.  
165 Smaller cats kill their prey by fast spine or head bites whereas bigger felids usually  
166 suffocate their prey sustaining throat or muzzle bite (Leyhausen and Tonkin, 1979;  
167 MacDonald, 2009; Kitchener et al., 2010). Within the *Panthera* lineage, the jaguar  
168 (*Panthera onca*) shows a specific sustained lethal bite at the back of the skull  
169 (Schaller and Vasconcelos, 1978; Palmeira et al., 2008). Although skull morphology  
170 is correlated to the MPM/PBM ratio (Christiansen and Wroe, 2007), the performance  
171 of jaw muscles is not correlated with the felid predatory performance and prey choice

172 (Sicuro and Oliveira, 2011). Recent studies also demonstrate that the whole post-  
173 cranial musculature is relatively weaker in large felids compared to smaller species  
174 (Cuff et al., 2016a, 2016b). Therefore, the correlation between bite force and prey  
175 selection is not clear. The so-called predatory behavior depends on head, body and  
176 limb movements in relation to prey properties (Wroe et al., 2005; Chitwood et al.,  
177 2014; Cuff et al., 2016a, 2016b). Among these properties, prey mass and anti-  
178 predatory behaviors (e.g., weapon use) are major factors influencing prey capture  
179 and subduance by predators. The use of the fore limbs is well described in Felidae  
180 with (i) their retractile claws grabbing the prey, and (ii) elbow rotation helping with  
181 manipulating the prey (Gonyea and Ashworth, 1975; Gonyea, 1978; Andersson and  
182 Werdelin, 2003; Andersson, 2004; Meachen-Samuels and Van Valkenburgh, 2009a;  
183 Stanton et al., 2015; Cuff et al., 2016a; Viranta et al., 2016). Even though the  
184 vertebral column does not seem to be influenced by the felid diet (Randau et al.,  
185 2016, 2017), the hind limbs are more impacted by predator's body size and  
186 locomotor behavior (Martín-Serra et al., 2014). Following the correlation between  
187 body size and prey selection (Dickman, 1988; Labisky and Boulay, 1998; Carbone et  
188 al., 1999, 2007; Meachen-Samuels and Van Valkenburgh, 2009a, 2009b; Clements  
189 et al., 2014; Cuff et al., 2015), we hypothesize that the morphology of the whole  
190 postcranial system provides a functional advantage in those cases where bite  
191 performance is not sufficient to subdue prey, as demonstrated in several carnivorous  
192 vertebrates (Helfman and Clark, 1986; Fish et al., 2007; D'Amore et al., 2011;) (Fig.  
193 1).

194 Connecting the hind limb to the vertebral column, the sacroiliac articulation has a  
195 critical role in supporting the body and countering gravity, and in force transmission  
196 from the hind limbs to the spine. This diarthrodial joint shape and its movements have  
197 been well documented in humans in relationship with bipedalism and parturition  
198 (Brooke, 1924; Weisl, 1955; Egund et al., 1978; Stuessen et al., 1989; Jesse et al.,  
199 2017). Although the evolution of the pelvis girdle is well documented in mammals  
200 (Romer, 1950; Ahlberg and Milner, 1994; Carroll, 2001; Gillis and Blob, 2001; Bejder  
201 and Hall, 2002; Kardong, 2002), there have been very few relevant studies on the  
202 sacroiliac joint in animals. Some studies have focused on the sacroiliac joint in  
203 horses in relationship to locomotor performance (Dalín and Jeffcott, 1986a, 1986b;  
204 Ekman et al., 1986; Erichsen et al., 2002; Dyson and Murray, 2003; Dyson et al.,  
205 2003a, 2003b). This joint is usually described as auricular shaped with wave-like

206 surfaces and without osseous contouring to support the maintenance of joint integrity  
207 as in ball-and-socket joints (Barone, 1986; Dalin and Jeffcott, 1986a, 1986b; Jesse et  
208 al., 2017). Its range of motion is reported to be very low (Weisl, 1955; Brooke, 1924;  
209 Barone, 1986; Dalin and Jeffcott, 1986a; Sturesson et al., 1989).

210 To date, the association between anatomical properties of the sacroiliac joint and  
211 behavioral and ecological factors has not been explored. The purpose of the present  
212 study is to investigate morphological properties of the iliac auricular surface in extant  
213 felids and to understand how body mass and ecological factors have impacted its  
214 shape. We predict that increase in felid body size is correlated with increase in  
215 stiffness of the sacroiliac joint. Furthermore, we predict that enhanced interlocking  
216 properties are correlated with increased speed and that gliding properties are  
217 correlated with climbing abilities. We also expect that joint stiffness could be  
218 correlated with selection of big prey. These analyses will allow us to propose a  
219 functional understanding of the biomechanics of the sacroiliac joint and the effects of  
220 felid size, locomotion and ecology on its shape.

221

## 222 **2. Material**

223 Coxal bones from 68 adult individuals were investigated in 12 species of Felidae  
224 (Table 1). All specimens were adults to avoid the effects of ontogenic variation and  
225 predominantly of wild caught origin. Properly disarticulated pelvises were selected.  
226 Joints showing arthritis were excluded from the sample. Specimens were all obtained  
227 from the collection Mammifères et Oiseaux at the Museum national d'Histoire  
228 naturelle (MNHN, Paris, France).

229

## 230 **3. Methods**

### 231 **3.1. General Morphology**

232 Each pelvis bone was examined and photographed with a Canon EOS 5D Mark III  
233 camera using a Canon lens EF 50mm 1:1.4. Coxal and sacral bone were pictured in  
234 a joint position in anterior, cranio-ventral, dorsal, and lateral views. Each coxal bone  
235 was separately pictured in cranio-ventral, dorsal, and lateral views. Standardized  
236 medial views of iliac auricular surface were not possible due to superposition by the  
237 contralateral iliac wing; therefore medio-ventral views of the auricular surfaces were  
238 taken. From these views and using CT-scan 3D reconstructions, it was possible to

239 create a morphological description of the auricular surfaces. All specimens were  
240 scanned at the CERMEP Imagerie du vivant (Bron, France) with a Siemens  
241 Healthcare mCT/S 64. Coxal bones were positioned with pubic tubercle and ventral  
242 iliac spine touching the CT-scan bed, and with the median plane of the scanner  
243 meeting the median plane of the bones, through the pubic symphysis.

244

### 245 **3.2. Geometric morphometric analyses**

246 In this analysis of the overall shape of the articulation, we used geometric  
247 morphometric approaches (Zelditch et al., 2012) and selected the auricular surfaces  
248 of the right and left ilium of each specimen. Right and left data were determined and  
249 tested separately. The three dimensional shape of the surfaces was studied by using  
250 eleven digitized anatomical landmarks (Fig. 2) defined in Table 2. The x, y and z  
251 landmark coordinates were acquired with a 3D Revware Microscribe system  
252 (Microscribe Utility Software 5.1). Once all landmark data were obtained, a  
253 generalized Procrustes superimposition (Rohlf and Slice, 1990) was performed by  
254 using the package RMORPH (Baylac, 2012) in R (R Core Team, 2014). Finally, a  
255 Principal Component Analysis (PCA) was performed on the shape data to evaluate  
256 the distribution of the species in morphospace. PCA scores keeping 90% of the  
257 overall shape variation were subsequently used as input for our comparative analysis  
258 (Baylac and Friess, 2005). MANOVA was performed using PCA scores to evaluate  
259 the effects of the following factors on the overall shape variability: lineage, body  
260 mass, locomotor behavior, prey selection represented by maximal average prey  
261 mass / average predator mass ratio (MPM/PBM), hunting strategy, and bite location  
262 (Table 1). In order to separate felids body mass into two classes (above and below  
263 14.5 kg), a minimal threshold of 14.5 kg, from which Carnivores switch to select  
264 bigger prey, was determined (Carbone et al., 2007). Based on data from Sicuro and  
265 Oliveira (2011), the MPM/PBM ratio for studied species was classified as follow: (i)  
266 ratio 1  $\geq 1.9$  (predators able to kill prey almost the double of their mass), (ii) ratio 2  
267 between 1 – 1.7 (predators able to kill prey around their own mass and up to 70%  
268 over their own mass), and (iii) ratio 3  $< 0.9$  (predators only able to kill prey lighter  
269 than themselves). When any significant difference was obtained on MANOVA  
270 analyses of PCA axes, ANOVA followed by post-hoc Tukey tests as the single-step  
271 multiple comparison procedure was used on first and second axis. Statistical

272 significance was set at p-value < 0.05 and the Bonferroni adjustment (Shaffer, 1995;  
273 Perneger, 1998; Rupert Jr, 2012;) was calculated at p-value = 0.007.

274

### 275 **3.3. Topographic variables**

276 Geometric morphometric provides a comprehensive description of the general shape  
277 of the iliac auricular surface and tests the differences between lineages in addition to  
278 some key ecological factors. However, the range of motion in this joint is known to be  
279 low and the wave shaped surfaces do not suggest gliding properties (Brooke, 1924;  
280 Weisl, 1955; Barone, 1986; Stuesson et al., 1989). Therefore, we assumed that the  
281 depth of the waves present on the auricular surfaces and the topography of its  
282 contours could play a key role in interlocking properties between the ilium and the  
283 sacrum and that these interlocking could play a functional role in connecting the hind  
284 limb to the spine. Regardless of all of other morphological features of the joint (e.g.,  
285 ligaments, muscles), we *a priori* speculated that interlocking abilities increased with  
286 the depth of the waves described on auricular surfaces. In contrast, smoother  
287 surfaces with smaller shallower waves could favor gliding movements. Therefore, we  
288 investigated the auricular surfaces topography to analyse interlocking abilities of the  
289 joint. To perform quantitative comparisons of topographic variables, we developed a  
290 new method to calculate the relative difference in level ( $d\%$ ) of landmarks to the  
291 reference plane including landmarks 2, 3 and 4 (Appendix 1, Fig. 2). We described  
292 the topography within the auricular surface with the series of landmarks 1, 9, 10, 11  
293 and 5. We defined an inner line with the line connecting these landmarks. The series  
294 of landmarks 2, 1, 8, 7, 6, 5 and 4 described the outline of the auricular surface and  
295 the line connecting these landmarks defined the outer line. From raw data, we  
296 calculated a 95% confidence interval for each landmark in each species and used  
297 this data set. We tested the effect of ecological factors on the level of landmark  
298 differences. For this, we selected those factors that were significant from the  
299 MANOVA results (see section Geometric morphometric analyses); i.e., body mass  
300 classes and MPM/PBM classes. Two classes of MPM/PBM ratio were used as  
301 determined from morphometric analyses: (i) a class defined by  $MPM/PBM < 1$  (ratio  
302 class 3, Table 1) including Domestic cat and Caracal lineages killing their prey with a  
303 spine bite, (ii) a class defined by  $MPM/PBM \geq 1$  (ratio classes 1 and 2, Table 1)  
304 including all other lineages that kill prey by suffocation or bite at the back of the skull.  
305 We tested these ecological factors on auricular surfaces topography by using a

306 Mann-Whitney test. Based on our result, simple descriptive analyses permit to  
307 identify the shapes of the inner and outer lines. All statistical analyses were  
308 performed in R. The significant level was selected at p-value < 0.05.

309

## 310 **4. Results**

### 311 **4.1. General Morphology**

312 The sacroiliac junctions are located between the coxal bones and the sacrum on  
313 either side of the midline of coxal and sacral bones (Fig. 3). On the coxal bone, the  
314 examined auricular surface was on the medial surface of the iliac wing (Fig. 4a), at  
315 half of its length, just cranial to the greater sciatic notch (Fig. 4f). The surface covered  
316 almost all the iliac height. As described by Jesse et al. (2017) for the human auricular  
317 surface shape, the outline separated the iliac auricular surface into two limbs: a  
318 dorsal limb and a ventral limb (Fig. 4b,c). At the junction between the two limbs, on  
319 the cranial edge of the joint, a central eminence was consistently found (Fig. 4d).  
320 Generally, joint surfaces were ear-shaped (i.e. auricular surface) with irregular  
321 outlines. The concave border was facing cranially. Most of the auricular surfaces did  
322 not show any division, but in some cases, the two limbs were completely or  
323 incompletely divided (Fig. 5). Three different outline shapes were described by Dalin  
324 and Jeffcott (1986a) for the iliac auricular surface in horses: (i) a “sock-shape” for the  
325 majority of studied horses, (ii) a “C-shape” (i.e. auricular), and (iii) a shape without  
326 much curvature (i.e. spatulate). In humans, Jesse et al. (2017) described similar  
327 shapes: (i) type 1 called “scone-shaped”, (ii) type 2 so called “auricle-shaped”, and  
328 (iii) type 3 called “crescent-shaped” (Fig. 5). In Felidae, six types of shape were  
329 visually defined according to their frequency as following (Fig. 5): type 1 (“auricle-  
330 shape”) was found in 59 cases (43.38%), type 2 (“crescent-shape”) in 30 cases  
331 (22.06%), type 3 (“spatula-shape”) in 17 cases (12.5%), type 4 (“bifoliate-shape”) in  
332 13 cases (9.56%), type 5 (“B-shape”) in 9 cases (6.62%), and type 6 (“Phrygian cap-  
333 shape”) in 8 cases (5.88%). For most specimens, similar shapes were found on each  
334 iliac bone, but in some cases shapes of right and left iliac surfaces were different  
335 (i.e., 7 *Panthera pardus*, 5 *Panthera tigris*, 5 *Panthera leo*, and 2 *Panthera onca*).  
336 The surfaces of dorsal and ventral limbs were generally concave. The area around  
337 the central eminence separating the joint limbs was generally lightly convex. Irregular  
338 wave-like striations marked the auricular surface in general, but the orientation of

339 these striations was not regular (Fig. 6). An elevated ridge along the dorso-caudal  
340 border of the iliac surface increased the concavity of the auricular surface (Fig. 4e, 6).  
341 The shape of this margin studied in frontal and transversal CT-Scan slides showed  
342 different outlines and different relief shapes among studied species (Fig. 7). In  
343 *Panthera* lineage species, the auricular surface covered the dorso-caudal ridge and  
344 formed a prominent crest offering a dorso-caudally convex articular surface to the  
345 sacrum. CT-scan transverse cuts of the dorsal limb articular surface in *Panthera*  
346 species showed an S-shape as opposed to a C-shape found in other felid species  
347 (Fig. 8).

348

## 349 **4.2. Geometric morphometrics**

### 350 **4.2.1. Lineages**

351 Figure 9 represents PCAs of the right and the left iliac auricular surfaces. The first  
352 two PCs of the right ilium account for 41% of the total shape variation (27% for PC1  
353 and 14% for PC2). The overall distribution defined by PCA scores explains 90% of  
354 the overall shape variation, and is significantly influenced by felid lineages  
355 (MANOVA, Pillai trace = 1.61;  $F = 3.42$ ;  $ddl = 4,44$ ;  $p\text{-value} < 0.007$ ). Post-hoc Tukey  
356 tests separated two lineages (Caracal and Domestic cat) from all other lineages  
357 (*Panthera*, *Lynx* and *Puma*) along PC1, whereas the Caracal lineage was separated  
358 from all other lineages along PC2. The first two PCs of the left ilium account for 36%  
359 of the total shape variation (19% for PC1 and 17% for PC2). The overall distribution  
360 defined by PCA scores explaining 90% of the overall shape variation tends to be  
361 significantly influenced by felid lineages (MANOVA, Pillai trace = 1.55;  $F = 2.91$ ;  $ddl =$   
362  $4,48$ ;  $p\text{-value} < 0.007$ ). Along PC1, the post-hoc Tukey test shows that Caracal  
363 belongs to two groups: one group involving Caracal and Domestic cat, and the other  
364 group involving Caracal, *Panthera*, *Lynx* and *Puma* lineages. Caracal lineage seems  
365 to be intermediate. Along PC2, Caracal is significantly different from all other lineages  
366 (Table 3). The post-hoc Tukey test shows diversity of the results based on the left  
367 and right iliac auricular surfaces.

368

### 369 **4.2.2. Locomotor behavior**

370 When the cheetah was classified as cursorial, locomotor behavior had no significant  
371 effect on joint shape (right joint: MANOVA, Pillai trace = 0.67;  $F = 1.45$ ;  $ddl = 3,33$ ;  $p\text{-}$   
372  $value = 0.07$ ; left joint: MANOVA, Pillai trace = 0.76;  $F = 1.56$ ;  $ddl = 3,36$ ;  $p\text{-value} =$

373 0.03). We obtained the same result when the cheetah was classified as a terrestrial  
374 felid (right joint: MANOVA, Pillai trace = 0.37; F = 1.15; ddl = 2,22; p-value = 0.30; left  
375 joint: MANOVA, Pillai trace = 0.58; F = 1.86; ddl = 2,24; p-value = 0.02).

376

### 377 **4.2.3. Body mass and predation**

378 The overall distribution defined by PCA scores explaining 90% of the overall shape  
379 variation and is significantly influenced by weight classes suggested by Carbone et  
380 al. (2007) for right (MANOVA, Pillai trace = 0.48; F = 4.74; ddl = 1,11; p-value <  
381 0.007) and left auricular surfaces (MANOVA, Pillai trace = 0.49; F = 4.38; ddl = 1,12;  
382 p-value < 0.007). The MPM/PBM ratio had a significant effect on the distribution  
383 describing the shape of the right ilium (MANOVA, Pillai trace = 0.92; F = 4.32; ddl =  
384 2,22; p-value < 0.007) and the shape of the left ilium (MANOVA, Pillai trace = 0.82; F  
385 = 3.21; ddl = 2,24; p-value < 0.007). The post-hoc Tukey test separated two ratio  
386 classes (1 and 2) from ratio class 3 for PC1 whereas the ratio had no significant  
387 effect for PC2 on both iliums (Table 3). Hunting strategy (solitary vs pack) neither  
388 showed any influence on the right (MANOVA, Pillai trace = 0.34; F = 2.58; ddl = 1,11;  
389 p-value = 0.01) nor on the left (MANOVA, Pillai trace = 0.30; F = 1.99; ddl = 1,12; p-  
390 value = 0.04) auricular shape. The type of bite had a significant effect on the overall  
391 distribution of PCA scores keeping 90% of the overall shape variation describing the  
392 right ilium (MANOVA, Pillai trace = 0.60; F = 2.21; ddl = 2,22; p-value < 0.006) but  
393 there was no significant effect on the shape of the left ilium (MANOVA, Pillai trace =  
394 0.59; F = 1.91; ddl = 2,24; p-value = 0.01). The post-hoc Tukey test separated  
395 suffocating bites and *Panthera onca*'s bite at the back of the skull from the spine bite  
396 for PC1. The bite had no significant effect for PC2 for the right ilium (Table 3)  
397 showing that *Panthera onca* was not different from all other big cats.

398

### 399 **4.3. Topography of the iliac auricular surface**

400 Table 4 presents statistical results of factors tested on landmark levels. The body  
401 mass had a significant effect on the height of all landmarks except for that on  
402 landmark 9. Except for landmark 11, ratio classes showed a significant effect on all  
403 landmarks. Figures 10 and 11 present the shape of the inner and the outer lines  
404 defined in methods for body mass and MPM/PBM ratio classes. The outer ridge of  
405 the surface is higher in big cats (with a body mass over 14.5 kg) compared to small  
406 cats, and for felids with MPM/PBM  $\geq 1$  compared to felids with MPM/PBM < 1. Two

407 shapes were identified to describe the inner topography of the surface. A W-shape is  
408 clearly determined in big cats with  $MPM/PBM \geq 1$ . A C-shape is identified in small  
409 cats with  $MPM/PBM < 1$ .

410

## 411 **5. Discussion**

### 412 **5.1. General Morphology**

413 In Felidae, the shape of iliac auricular surface showed an unexpected diversity that  
414 we can relate to various behaviors, primarily the predatory behavior. Whereas the  
415 literature described only three shapes up to date in mammals (Dalin and Jeffcott,  
416 1986a; Jesse et al., 2017), six different shapes were found in the studied Felidae  
417 species (Fig. 5). The topography of the surface, with wave-like striations oriented in  
418 different directions, probably limits the gliding properties of the surface (Fig. 6). In the  
419 *Panthera* lineage, the articular surface covered the dorso-caudal ridge enhancing the  
420 general wave-like surface topography (Fig. 6-8). Functionally, this surface offers a  
421 bone-to-bone contact between ilium and sacrum when there is posterior movement of  
422 iliac wing. Without this connection, during posterior pull on the sacrum by the coxal  
423 bone, the sacrum would follow due to tension the sacro-iliac ligaments. Therefore,  
424 this particular connection between sacral and iliac bones facilitates the transmission  
425 of a posterior movement of the pelvis in relation to the spine. This transmission is not  
426 used during propulsive efforts during locomotion but occurs specifically during  
427 backwards motion. We consider that such morphological feature could provide a  
428 functional benefit for subduing bigger prey in accordance with observed felid  
429 postures (Fig. 1).

430

431 Despite the variability of the post-hoc Tukey test results on the right and left surfaces,  
432 overall PCAs separated Caracal and Domestic cat lineages from all other lineages  
433 (Table 3). Phylogenetically, these two lineages were separated approximately 15  
434 million years ago (Nyakatura and Bininda-Emonds, 2012). Based on their  
435 phylogenetic relationships, Domestic cat lineage is much closer to Puma and Lynx  
436 lineages than to the Caracal lineage. Predatory traits of Felidae have been debated  
437 for a long time in the context of their phylogeny (Collier and O'Brien, 1985; Mattern  
438 and McLennan, 2000; Bininda-Emonds et al., 2001; Yu and Zhang, 2005; Werdelin et  
439 al., 2010). For example, Cuff et al. (2015) suggest that phylogeny underlies felid body

440 mass evolution with prey selection preference. But, Parés-Casanova and de la Cruz  
441 (2017) suggest that biomechanics, not necessarily phylogeny, explain cranial  
442 variables. This differentiation between lineages not following updated phylogenies  
443 suggests that other factors, including constraints linked to predation, influence the  
444 iliac auricular shape in this clade of mammals.

445

446 The body mass threshold of 14.5 kg determined by Carbone et al. (2007) had a  
447 significant effect on the iliac auricular shape. In our study, this threshold separates  
448 Domestic cat, Caracal and Lynx lineages from all other lineages (Table 3).  
449 Unsurprisingly, increase in stiffness of the joint linking the hind limb to the body offers  
450 better support to the spine, which is an important requisite when considering  
451 increasing in body mass.

452

453 Our classification of prey selection based on MPM/PBM ratio (Table 1) also showed a  
454 significant effect on the auricular surface shape separating ratio class 3 (Caracal and  
455 Domestic cat lineages) from ratio classes 1 and 2 (Table 3). Considering the ability to  
456 catch prey lighter or heavier than their own weight (ratio class 3 vs ratio classes 1  
457 and 2), Caracal and Domestic cat lineages are still separated from all other lineages  
458 considered in the current study. In contrast to body mass classes, where Lynx falls  
459 within small prey specialists, ratio classification separated *Lynx sp.* Furthermore, bite  
460 location also separated felids killing their prey with a spine lethal bite from felids using  
461 suffocation or crushing the back of the skull to kill their prey. Again, *Domestic cats*  
462 and *Caracal* lineages species representing the spine bite are separated from all other  
463 felids. However, *Panthera onca* is the only species killing prey with a sustained bite at  
464 the back of the skull among all Felidae species. Due to this behavioral uniqueness,  
465 when comparing this species to all other species of the sample, the MANOVA might  
466 not be able to detect the characteristics that are different between the jaguar and  
467 other species. Furthermore, pack or solitary hunting strategies had no significant  
468 effect on the iliac auricular shape suggesting that the joint is shaped by individuals'  
469 ability to select small or big prey. Again, there is only one representative of regular  
470 pack hunting among Felidae species and the difference in the auricular shape  
471 between the lion and all other species might not be detected by the MANOVA.  
472 Nevertheless, all these results suggest that the effect of the body weight on the  
473 shape of the sacroiliac joint is probably related to postures and movements that big

474 felids perform during hunting large prey, with an absence of the effect in smaller  
475 felids which are mostly unable to bring down big prey.

476

477 No locomotor class had significant effect on the overall shape of the iliac auricular  
478 surface. This unexpected result suggest that body mass and predation might be the  
479 main stressors to drive the auricular surface shape. This joint biomechanics seem to  
480 have potential abilities to answer to all constraints due to felids locomotor behaviors.  
481 Interestingly, the three locomotor classes (i.e., terrestrial, scansorial, and arboreal)  
482 used by several authors do not differentiate felids locomotor behavior on quantitative  
483 data (Meachen-Samuels and Van Valkenburgh, 2009a; Randau et al., 2016). Indeed,  
484 all felids are able to run high speed (Garland and Janis, 1993) or to climb trees. Even  
485 when cheetah (*Acinonyx jubatus*) is separated from all other felids as cursorial  
486 (Martín-Serra et al., 2014) these classes have no effect on the morphological  
487 characteristics of the joint linking the hind limbs to the spine. Further studies may find  
488 other locomotor stressors that could impact on the auricular surface shape.

489

## 490 **5.2. Topography of the iliac auricular surface**

491 We investigated iliac auricular surface topography to evaluate joint interlocking  
492 properties. Our results show that all landmarks on the outer line (landmarks 5, 6, 7, 8)  
493 and all landmarks but one on the inner line (landmarks 10,11, 5 for body mass  
494 classes and landmarks 9, 10, 5 for MPM/PBM ratio classes) of the auricular surface  
495 shape have a significant level difference (Table 4) resulting in a more complex  
496 surface for cats over 14.5 kg or with MPM/PBM ratio  $\geq 1$  (Fig. 10 and 11). Indeed this  
497 difference of topography describes a higher ridge and deeper waves in the joint of big  
498 cats with larger MPM/PBM ratios (Fig. 10 and 11). In these cats, especially in the first  
499 case, the inner line connecting landmarks 1, 9, 10, 11 and 5 draws a W-shape (Fig.  
500 10 and 11). Such a shape probably prevents gliding between the ilium and the  
501 sacrum in the dorsoventral direction, enhancing the interlocking ability and potentially  
502 leading to rigidity in the joint (Fig. 12). In small cats, the same line presents a C-  
503 shape (Fig. 10 and 11) and the topography may allow further mobility between iliac  
504 and sacral bones. Furthermore, all landmarks are higher along the outline in big cats  
505 than in small cats (Fig. 10 and 11) building a more elevated ridge and limiting the  
506 movements of the sacrum between the iliac wings. The dorso-caudal part of this

507 ridge is covered by the articular surface in *Panthera* lineage species and prevents  
508 any dorso-ventral gliding of the sacrum (Fig.12).

509

510 This increase in interlocking ability can also optimize several morphological features  
511 recorded in big cats. Sicuro and Oliveira (2011) emphasize that the performance of  
512 jaw muscles is not correlated with the MPM/PBM ratio. Furthermore, Cuff et al.  
513 (2016) state that the limbs and lumbosacral muscles weaken with an increase in  
514 body mass. Even though myofascial chains are involved in force transmission  
515 (Krause et al., 2016), these findings support that articulations might play an active  
516 role in stabilizing the spine in large species. Randau et al. (2017) suggest that an  
517 increased height of the vertebral centrum of the cervical and thoracic vertebrae  
518 enhanced the spine stability in the dorsoventral plane. Such passive stiffness is not  
519 observed in the lumbar region, except for L7 which articulates with the sacrum. The  
520 pre-sacral vertebral column (i.e. T10-L7) is more correlated with body size and  
521 ecological traits than the rest of the spine (Randau et al., 2016). Specialization in  
522 prey size is the only ecological factor showing a significant correlation with the total  
523 vertebral column shape (Randau et al., 2016). Based on this set of factors related to  
524 the size and the prey selection in big cats, an empirical functional model of predatory  
525 felid behavior can be proposed. While biting, big cats support themselves using the  
526 ground or the prey itself (Fig. 1). Front and hind limbs push the body backwards while  
527 the jaw maintains the bite on the struggling prey. From this starting position, hind  
528 limbs are flexed under the body as in a crouching posture and lumbar column is  
529 flexed. When pulling on the prey, the strength from the hind limbs on the ground is  
530 transmitted to the hip. Hind limbs extend backwards causing the lumbar column to  
531 extend too; all of this causes the pelvis to move backwards as well, transmitting its  
532 momentum to the head through the spine. The increased interlocking of the sacroiliac  
533 junction facilitates a full transmission of this momentum. Stiffness at the lumbosacral  
534 junction, thoracic and cervical joints, increases the stability of the column and  
535 improves force transmission. In this model, the backwards movement of the  
536 postcranial musculoskeletal system optimizes the hunting mode by increasing the  
537 force used by the head while biting.

538

## 539 **6. Conclusion**

540 From small to big cats, body mass is a major factor impacting postcranial  
541 musculoskeletal properties and prey selection. At the junction between hind limbs  
542 and vertebral column, the sacroiliac joint is crucially influenced by body mass and  
543 other ecological stressors. In bigger cats that are able to kill prey heavier than their  
544 own weight, the topography of the iliac auricular surface shows complex shapes  
545 increasing interlocking properties and stiffness. This enhanced stiffness is necessary  
546 to support heavier body mass but also to manage predatory stressors; this is not the  
547 case of locomotion. The morphology of the iliac auricular surface of felids feeding on  
548 large prey is significantly different to the one of felids feeding on small prey; W-shape  
549 versus C-shape respectively for the inner line and a more elevated border of the  
550 outer line for the former group. Additionally, in the *Panthera* lineage species, an  
551 extension of the auricular surface on the caudal ridge of the joint builds a bone-to-  
552 bone interlocking system between iliac and sacrum bones during pelvis posterior  
553 motion. According to these results, it can be inferred that sacroiliac morphology in  
554 larger cats provides a functional advantage in subduing large prey by transmitting a  
555 momentum from the rear to the head during the struggle and probably plays a key  
556 role in predator success. Other morphological and functional properties of the  
557 articulation (e.g. position in the pelvis, ligament and muscular systems) remain to be  
558 investigated more deeply.

559

## 560 **Acknowledgements**

561

562 The authors thank the following financial supports of this study: (i) ATMs – Muséum  
563 national d'Histoire naturelle 2013-2015 "*Formes possibles, Formes réalisées...*" (Dir:  
564 Pr Vincent Bels & Pr Pierre-Henri Gouyon), and (ii) UMR 7205 (Dir: Dr CNRS  
565 Philippe Grancolas). We are grateful to Pr Luc Zimmer who allowed us to use the  
566 "*Centre d'Etude et de Recherche multimodale en imagerie du Vivant*" (CERMEP,  
567 CNRS – INSB) for all of the CT-scans used in this study and to Franck Lambertson for  
568 his help and coordination on the platform. We are grateful to Carole Czmil, Nathalie  
569 Moshfegh and Arina Nussberger for the English review and to Jérôme Curty for his  
570 support in DTP. We thank two anonymous reviewers for their highly helpful  
571 comments on this paper

572

573

## 574 **Authors contributions**

575 JPP performed the study and wrote the paper. RC did the whole geometric  
576 morphometric, and wrote the paper. MAP provided the whole technical support  
577 needed for all analyses. EP provided the support and help needed to work with the  
578 collections of the Museum. FL did the CT-scans. VA did all the calculations to  
579 compare some of the morphological data. MR did the statistic descriptive analyses.  
580 VB wrote the paper.

581 The authors declare no conflict of interest.

582

## 583 **References**

584

- 585 Ahlberg, P.E., Milner, A.R., 1994. The origin and early diversification of tetrapods.  
586 *Nature* 368, 507.
- 587 Andersson, K.I., 2004. Elbow-joint morphology as a guide to forearm function and  
588 foraging behaviour in mammalian carnivores. *Zool. J. Linn. Soc.* 142, 91–104.
- 589 Andersson, K.I., Werdelin, L., 2003. The evolution of cursorial carnivores in the  
590 Tertiary: implications of elbow-joint morphology. *Proc. R. Soc. Lond. B Biol.*  
591 *Sci.* 270, S163–S165.
- 592 Bailey, I., Myatt, J.P., Wilson, A.M., 2013. Group hunting within the Carnivora:  
593 physiological, cognitive and environmental influences on strategy and  
594 cooperation. *Behav. Ecol. Sociobiol.* 67, 1–17.
- 595 Barone, R., 1986. Anatomie comparée des Mammifères domestiques, tome 2,  
596 Arthrologie et myologie. Vigot Freres Paris.
- 597 Baylac, M., 2012. Rmorph: a R geometric and multivariate morphometrics library.  
598 Available Author Baylac Mnhn Fr.
- 599 Baylac, M., Friess, M., 2005. Fourier descriptors, Procrustes superimposition, and  
600 data dimensionality: an example of cranial shape analysis in modern human  
601 populations, in: *Modern Morphometrics in Physical Anthropology*. Springer, pp.  
602 145–165.
- 603 Bejder, L., Hall, B.K., 2002. Limbs in whales and limblessness in other vertebrates:  
604 mechanisms of evolutionary and developmental transformation and loss. *Evol.*  
605 *Dev.* 4, 445–458.
- 606 Bertram, J.E., Biewener, A.A., 1990. Differential scaling of the long bones in the  
607 terrestrial Carnivora and other mammals. *J. Morphol.* 204, 157–169.
- 608 Biewener, A., 1989. Scaling body support in mammals: limb posture and muscle  
609 mechanics. *Science* 245, 45–48.
- 610 Biewener, A., Patek, S., 2018. *Animal locomotion*. Oxford University Press.
- 611 Bininda-Emonds, O.R., Decker-Flum, D.M., Gittleman, J.L., 2001. The utility of  
612 chemical signals as phylogenetic characters: an example from the Felidae.  
613 *Biol. J. Linn. Soc.* 72, 1–15.
- 614 Brooke, R., 1924. The sacro-iliac joint. *J. Anat.* 58, 299.
- 615 Carbone, C., Mace, G.M., Roberts, S.C., Macdonald, D.W., 1999. Energetic  
616 constraints on the diet of terrestrial carnivores. *Nature* 402, 286.
- 617 Carbone, C., Teacher, A., Rowcliffe, J.M., 2007a. The costs of carnivory. *PLoS Biol*  
618 5, e22.

619 Caro, T., 1994. Cheetahs of the Serengeti Plains: group living in an asocial species.  
620 University of Chicago Press.

621 Caro, T., Fitzgibbon, C.D., 1992. Large carnivores and their prey: the quick and the  
622 dead. *Nat. Enemies Popul. Biol. Predat. Parasites Dis.* 115–142.

623 Carroll, R.L., 2001. The origin and early radiation of terrestrial vertebrates. *J.*  
624 *Paleontol.* 75, 1202–1213.

625 Chitwood, M.C., Lashley, M.A., Moorman, C.E., DePerno, C.S., 2014. Confirmation  
626 of coyote predation on adult female white-tailed deer in the southeastern  
627 United States. *Southeast. Nat.* 3, N30–N32.

628 Christiansen, P., Wroe, S., 2007. Bite forces and evolutionary adaptations to feeding  
629 ecology in carnivores. *Ecology* 88, 347–358.

630 Clements, H.S., Tambling, C.J., Hayward, M.W., Kerley, G.I., 2014. An objective  
631 approach to determining the weight ranges of prey preferred by and  
632 accessible to the five large African carnivores. *PLoS One* 9, e101054.

633 Collier, G.E., O'Brien, S.J., 1985. A molecular phylogeny of the Felidae:  
634 immunological distance. *Evolution* 39, 473–487.

635 Cuff, A.R., Randau, M., Head, J., Hutchinson, J.R., Pierce, S.E., Goswami, A., 2015.  
636 Big cat, small cat: reconstructing body size evolution in living and extinct  
637 Felidae. *J. Evol. Biol.* 28, 1516–1525. <https://doi.org/10.1111/jeb.12671>

638 Cuff, A.R., Sparkes, E.L., Randau, M., Pierce, S.E., Kitchener, A.C., Goswami, A.,  
639 Hutchinson, J.R., 2016a. The scaling of postcranial muscles in cats (Felidae) I:  
640 forelimb, cervical, and thoracic muscles. *J. Anat.* 229, 128–141.

641 Cuff, A.R., Sparkes, E.L., Randau, M., Pierce, S.E., Kitchener, A.C., Goswami, A.,  
642 Hutchinson, J.R., 2016b. The scaling of postcranial muscles in cats (Felidae)  
643 II: hind limb and lumbosacral muscles. *J. Anat.* 229, 142–152.

644 Dalin, G., Jeffcott, L.B., 1986a. Sacroiliac joint of the horse 1. Gross morphology.  
645 *Anat. Histol. Embryol.* 15, 80–94.

646 Dalin, G., Jeffcott, L.B., 1986b. Sacroiliac joint of the horse 2. Morphometric features.  
647 *Anat. Histol. Embryol.* 15, 97–107.

648 D'Amore, D.C., Moreno, K., McHenry, C.R., Wroe, S., 2011. The effects of biting and  
649 pulling on the forces generated during feeding in the Komodo dragon  
650 (*Varanus komodoensis*). *PLOS One* 6, e26226.

651 Davidson, Z., Valeix, M., Van Kesteren, F., Loveridge, A.J., Hunt, J.E., Murindagomo,  
652 F., Macdonald, D.W., 2013. Seasonal diet and prey preference of the African  
653 lion in a waterhole-driven semi-arid savanna. *PLoS One* 8, e55182.

654 Day, L.M., Jayne, B.C., 2007. Interspecific scaling of the morphology and posture of  
655 the limbs during the locomotion of cats (Felidae). *J. Exp. Biol.* 210, 642–654.

656 Dickman, C.R., 1988. Body size, prey size, and community structure in insectivorous  
657 mammals. *Ecology* 69, 569–580.

658 Dyson, S., Murray, R., 2003. Pain associated with the sacroiliac joint region: a clinical  
659 study of 74 horses. *Equine Vet. J.* 35, 240–245.

660 Dyson, S., Murray, R., Branch, M., Whitton, C., Donovan, T., Harding, E., 2003a. The  
661 sacroiliac joints: evaluation using nuclear scintigraphy. Part 1: The normal  
662 horse. *Equine Vet. J.* 35, 226–232.

663 Dyson, S., Murray, R., Branch, M., Harding, E., 2003b. The sacroiliac joints:  
664 evaluation using nuclear scintigraphy. Part 2: Lamé horses. *Equine Vet. J.* 35,  
665 233–239.

666 Egund, N., Olsson, T.H., Schmid, H., Selvik, G., 1978. Movements in the sacroiliac  
667 joints demonstrated with roentgen stereophotogrammetry. *Acta Radiol. Diagn.*  
668 (Stockh.) 19, 833–846.

669 Ekman, S., Dalin, G., Olsson, S.-E., Jeffcott, L.B., 1986. Sacroiliac joint of the horse  
670 3. Histological appearance. *Anat. Histol. Embryol.* 15, 108–121.

671 Erichsen, C., Berger, M., Eksell, P., 2002. The scintigraphic anatomy of the equine  
672 sacroiliac joint. *Vet. Radiol. Ultrasound* 43, 287–292.

673 Fish, F.E., Bostic, S.A., Nicastro, A.J., Beneski, J.T., 2007. Death roll of the alligator:  
674 mechanics of twist feeding in water. *J. Exp. Biol.* 210, 2811–2818.

675 Garland, T., Janis, C.M., 1993. Does metatarsal/femur ratio predict maximal running  
676 speed in cursorial mammals? *J. Zool.* 229, 133–151.

677 Gillis, G.B., Blob, R.W., 2001. How muscles accommodate movement in different  
678 physical environments: aquatic vs. terrestrial locomotion in vertebrates. *Comp.*  
679 *Biochem. Physiol. A. Mol. Integr. Physiol.* 131, 61–75.

680 Gittleman, J.L., 2013. *Carnivore Behavior, Ecology, and Evolution*. Springer Science  
681 & Business Media.

682 Gonyea, W.J., 1978. Functional implications of felid forelimb anatomy. *Cells Tissues*  
683 *Organs* 102, 111–121.

684 Gonyea, W., Ashworth, R., 1975. The form and function of retractile claws in the  
685 Felidae and other representative carnivorans. *J. Morphol.* 145, 229–238.

686 Hayward, M.W., Jędrzejewski, W., Jędrzejewska, B., 2012. Prey preferences of the  
687 tiger *Panthera tigris*. *J. Zool.* 286, 221–231.

688 Hayward, M.W., Kerley, G.I., 2005. Prey preferences of the lion (*Panthera leo*). *J.*  
689 *Zool.* 267, 309–322.

690 Helfman, G.S., Clark, J.B., 1986. Rotational feeding: overcoming gape-limited  
691 foraging in anguillid eels. *Copeia* 679–685.

692 Janis, C.M., Figueirido, B., 2014. Forelimb anatomy and the discrimination of the  
693 predatory behavior of carnivorous mammals: the thylacine as a case study. *J.*  
694 *Morphol.* 275, 1321–1338.

695 Jesse, M.K., Kleck, C., Williams, A., Petersen, B., Glueck, D., Lind, K., Patel, V.,  
696 2017. 3D Morphometric Analysis of Normal Sacroiliac Joints: A New  
697 Classification of Surface Shape Variation and the Potential Implications in Pain  
698 Syndromes. *Pain Physician* 10.

699 Kardong, K.V., 2002. *Vertebrates: Comparative Anatomy, Function, Evolution*.  
700 McGraw-Hill New York.

701 Kitchener, A.C., Van Valkenburgh, B., Yamaguchi, N., Macdonald, D.W., Loveridge,  
702 A.J., 2010. Felid form and function. *Biol. Conserv. Wild Felids* 83–106.

703 Kleiman, D.G., Eisenberg, J.F., 1973. Comparisons of canid and felid social systems  
704 from an evolutionary perspective. *Anim. Behav.* 21, 637–659.

705 Kohl, K.D., Coogan, S.C., Raubenheimer, D., 2015. Do wild carnivores forage for  
706 prey or for nutrients? *BioEssays* 37, 701–709.

707 Krause, F., Wilke, J., Vogt, L., Banzer, W., 2016. Intermuscular force transmission  
708 along myofascial chains: a systematic review. *J. Anat.* 228, 910–918.

709 Labisky, R.F., Boulay, M.C., 1998. Behaviors of bobcats preying on white-tailed deer  
710 in the Everglades. *Am. Midl. Nat.* 139, 275–281.

711 Leyhausen, P., Tonkin, B.A., 1979. *Cat behaviour. The predatory and social*  
712 *behaviour of domestic and wild cats*. Garland STPM Press.

713 MacDonald, D., 2009. *The Encyclopedia of Mammals*. OUP Oxford.

714 Machovsky-Capuska, G.E., Coogan, S.C., Simpson, S.J., Raubenheimer, D., 2016.  
715 *Motive for Killing: What Drives Prey Choice in Wild Predators?* *Ethology* 122,  
716 703–711.

- 717 MacNulty, D.R., Mech, L.D., Smith, D.W., 2007. A proposed ethogram of large-  
718 carnivore predatory behavior, exemplified by the wolf. *J. Mammal.* 88, 595–  
719 605.
- 720 Martin, L.D., 1989. Fossil history of the terrestrial Carnivora, in: *Carnivore Behavior,*  
721 *Ecology, and Evolution.* Springer, pp. 536–568.
- 722 Martín-Serra, A., Figueirido, B., Palmqvist, P., 2014. A three-dimensional analysis of  
723 the morphological evolution and locomotor behaviour of the carnivoran hind  
724 limb. *BMC Evol. Biol.* 14, 129.
- 725 Mattern, M.Y., McLennan, D.A., 2000. Phylogeny and speciation of felids. *Cladistics*  
726 16, 232–253.
- 727 Meachen-Samuels, J., 2010. Comparative scaling of humeral cross-sections of felids  
728 and canids using radiographic images. *J. Mamm. Evol.* 17, 193–209.
- 729 Meachen-Samuels, J., Van Valkenburgh, B., 2009a. Forelimb indicators of prey-size  
730 preference in the Felidae. *J. Morphol.* 270, 729–744.
- 731 Meachen-Samuels, J., Van Valkenburgh, B., 2009b. Craniodental indicators of prey  
732 size preference in the Felidae. *Biol. J. Linn. Soc.* 96, 784–799.
- 733 Morales, M.M., Giannini, N.P., 2013. Ecomorphology of the African felid ensemble:  
734 the role of the skull and postcranium in determining species segregation and  
735 assembling history. *J. Evol. Biol.* 26, 980–992.
- 736 Morales, M.M., Giannini, N.P., 2014. Pleistocene extinctions and the perceived  
737 morphofunctional structure of the Neotropical felid ensemble. *J. Mamm. Evol.*  
738 21, 395–405.
- 739 Morales, M.M., Moyano, S.R., Ortiz, A.M., Ercoli, M.D., Aguado, L.I., Cardozo, S.A.,  
740 Giannini, N.P., 2018. Comparative myology of the ankle of *Leopardus wiedii*  
741 and *L. geoffroyi* (Carnivora: Felidae): functional consistency with osteology,  
742 locomotor habits and hunting in captivity. *Zoology* 126, 46–57.
- 743 Mukherjee, S., Heithaus, M.R., 2013. Dangerous prey and daring predators: a  
744 review. *Biol. Rev.* 88, 550–563. <https://doi.org/10.1111/brv.12014>
- 745 Nyakatura, K., Bininda-Emonds, O.R., 2012. Updating the evolutionary history of  
746 Carnivora (Mammalia): a new species-level supertree complete with  
747 divergence time estimates. *BMC Biol.* 10, 12.  
748 <https://doi.org/10.1186/PREACCEPT-5398900576110216>
- 749 Palmeira, F.B., Crawshaw Jr, P.G., Haddad, C.M., Ferraz, K.M.P., Verdade, L.M.,  
750 2008. Cattle depredation by puma (*Puma concolor*) and jaguar (*Panthera*  
751 *onca*) in central-western Brazil. *Biol. Conserv.* 141, 118–125.
- 752 Parés-Casanova, P.M., de la Cruz, S., 2017. Larger wild felids exhibit longer dental  
753 skeletons. *J. Zool. Biosci. Res.* 1.
- 754 Perneger, T.V., 1998. What's wrong with Bonferroni adjustments. *Bmj* 316, 1236–  
755 1238.
- 756 Piras, P., Silvestro, D., Carotenuto, F., Castiglione, S., Kotsakis, A., Maiorino, L.,  
757 Melchionna, M., Mondanaro, A., Sansalone, G., Serio, C., 2018. Evolution of  
758 the sabertooth mandible: A deadly ecomorphological specialization.  
759 *Palaeogeogr. Palaeoclimatol. Palaeoecol.*
- 760 Pulliam, H.R., Caraco, T., 1984. Living in groups: is there an optimal group size.  
761 *Behav. Ecol. Evol. Approach* 2, 122–147.
- 762 Radloff, F.G.T., Du Toit, J.T., 2004. Large predators and their prey in a southern  
763 African savanna: a predator's size determines its prey size range. *J. Anim.*  
764 *Ecol.* 73, 410–423. <https://doi.org/10.1111/j.0021-8790.2004.00817.x>

765 Randau, M., Goswami, A., Hutchinson, J.R., Cuff, A.R., Pierce, S.E., 2016. Cryptic  
766 complexity in felid vertebral evolution: shape differentiation and allometry of  
767 the axial skeleton. *Zool. J. Linn. Soc.* 178, 183–202.

768 Randau, M., Cuff, A.R., Hutchinson, J.R., Pierce, S.E., Goswami, A., 2017. Regional  
769 differentiation of felid vertebral column evolution: a study of 3D shape  
770 trajectories. *Org. Divers. Evol.* 17, 305–319.

771 Rohlf, F.J., Slice, D., 1990. Extensions of the Procrustes method for the optimal  
772 superimposition of landmarks. *Syst. Biol.* 39, 40–59.

773 Romer, A.S., 1950. *The vertebrate body*. WB Saunders Company; London.

774 Rothwell, T., 2003. Phylogenetic systematics of North American *Pseudaelurus*  
775 (Carnivora: Felidae). *Am. Mus. Novit.* 1–64.

776 Rudnai, J.A., 2012. *The Social Life of the Lion: A study of the behaviour of wild lions*  
777 (*Panthera leo massaica* [Newmann]) in the Nairobi National Park, Kenya.  
778 Springer Science & Business Media.

779 Rupert Jr, G., 2012. *Simultaneous statistical inference*. Springer Science & Business  
780 Media.

781 Samuels, J.X., Meachen, J.A., Sakai, S.A., 2013. Postcranial morphology and the  
782 locomotor habits of living and extinct carnivorans. *J. Morphol.* 274, 121–146.

783 Schaller, G.B., 2009. *The Serengeti lion: a study of predator-prey relations*. University  
784 of Chicago Press.

785 Schaller, G.B., Vasconcelos, J.M.C., 1978. Jaguar predation on capybara. *Z*  
786 *Säugetierk* 43, 296–301.

787 Scheel, D., Packer, C., 1991. Group hunting behaviour of lions: a search for  
788 cooperation. *Anim. Behav.* 41, 697–709.

789 Seidensticker, J., McDougal, C., 1993. Tiger predatory behaviour, ecology and  
790 conservation.

791 Shaffer, J.P., 1995. Multiple hypothesis testing. *Annu. Rev. Psychol.* 46, 561–584.

792 Sicuro, F.L., Oliveira, L.F.B., 2011a. Skull morphology and functionality of extant  
793 Felidae (Mammalia: Carnivora): a phylogenetic and evolutionary perspective.  
794 *Zool. J. Linn. Soc.* 161, 414–462.

795 Slater, G.J., Van Valkenburgh, B., 2009. Allometry and performance: the evolution of  
796 skull form and function in felids. *J. Evol. Biol.* 22, 2278–2287.

797 Stander, P.E., 1992. Cooperative hunting in lions: the role of the individual. *Behav.*  
798 *Ecol. Sociobiol.* 29, 445–454.

799 Stanton, L.A., Sullivan, M.S., Fazio, J.M., 2015. A standardized ethogram for the  
800 felidae: A tool for behavioral researchers. *Appl. Anim. Behav. Sci.* 173, 3–16.

801 Stuessen, B., Selvik, Gö., Udén, A., 1989. Movements of the sacroiliac joints. A  
802 roentgen stereophotogrammetric analysis. *Spine* 14, 162–165.

803 Sunquist, M., Sunquist, F., 2017. *Wild Cats of the World*. University of Chicago  
804 Press.

805 Sunquist, M.E., Sunquist, F.C., 1989. Ecological constraints on predation by large  
806 felids, in: *Carnivore Behavior, Ecology, and Evolution*. Springer, pp. 283–301.

807 Tirok, K., Bauer, B., Wirtz, K., Gaedke, U., 2011. Predator-prey dynamics driven by  
808 feedback between functionally diverse trophic levels. *PloS One* 6, e27357.

809 Viranta, S., Lommi, H., Holmala, K., Laakkonen, J., 2016a. Musculoskeletal anatomy  
810 of the Eurasian lynx, *Lynx lynx* (Carnivora: Felidae) forelimb: Adaptations to  
811 capture large prey? *J. Morphol.* 277, 753–765.

812 Weisl, H., 1955. The movements of the sacro-iliac joint. *Cells Tissues Organs* 23,  
813 80–91.

- 814 Werdelin, L., Yamaguchi, N., Johnson, W.E., O'Brien, S.J., 2010. Phylogeny and  
815 evolution of cats (Felidae). *Biol. Conserv. Wild Felids* 59–82.
- 816 Wroe, S., McHenry, C., Thomason, J., 2005. Bite club: comparative bite force in big  
817 biting mammals and the prediction of predatory behaviour in fossil taxa. *Proc.*  
818 *R. Soc. Lond. B Biol. Sci.* 272, 619–625.
- 819 Yu, L., Zhang, Y., 2005. Phylogenetic studies of pantherine cats (Felidae) based on  
820 multiple genes, with novel application of nuclear  $\beta$ -fibrinogen intron 7 to  
821 carnivores. *Mol. Phylogenet. Evol.* 35, 483–495.
- 822 Zelditch, M.L., Swiderski, D.L., Sheets, H.D., 2012. *Geometric Morphometrics for*  
823 *Biologists: A Primer.* Academic Press.
- 824 Zhang, K.Y., Wiktorowicz-Conroy, A., Hutchinson, J.R., Doube, M., Klosowski, M.,  
825 Shefelbine, S.J., Bull, A.M., 2012. 3D Morphometric and posture study of felid  
826 scapulae using statistical shape modelling. *PLoS One* 7, e34619.
- 827
- 828

829 **Figure legends**

830

831 Figure 1. Various felid killing postures in Felidae species showing cranial and post  
832 cranial systems involvement. A, Jungle cat (*Felis chaus*) killing a bird. After catching  
833 the prey, the bite force efficiency is enough to immobilize and kill a low weight prey.  
834 B, Leopard (*Panthera pardus*) immobilizing and killing a gazelle. To this end, the  
835 leopard uses its fore limbs to immobilize the prey on the ground while the back and  
836 the pelvis are flexed; hind limbs stabilize the predator on the ground. C, Female lion  
837 (*Panthera leo*) killing a young wildebeest on her own. Stabilization of this predator-  
838 prey system is give, by the lioness' actions of jaw closure, front limbs grabbing the  
839 prey and hind limbs pushing on the prey itself. D, Male lion (*Panthera leo*) preying on  
840 a buffalo. Killing such a huge prey for a lion requires a cooperative hunting. For this  
841 hunting, lion uses its bite, its front limbs to grab the prey and hind limbs to push, all of  
842 these acting together involving cranial and post-cranial elements.

843

844 Figure 2. A, Landmarks on *Panthera onca* right iliac auricular surface. All the  
845 landmarks were mirrored on the left ilium as defined in Table 2. Cd, caudal; Cr,  
846 cranial; D, dorsal; V, ventral. B, Measurements of the auricular surface relief.  $\vec{v}_n$  is a  
847 vector orthonormal to the plane including landmarks 2, 3 and 4. The method to  
848 calculate the difference in level of each landmark from the plane is explained in  
849 appendix I. Solid red line connecting landmarks 2, 1, 8, 7, 6, 5, and 4 defines the  
850 outer line. Dotted red line connecting landmarks 1, 9, 10, 11, and 5 defines the inner  
851 line.

852

853 Figure 3. Examples of felid pelvis showing the interlocking between the sacrum and  
854 the coxal bones in dorsal, cranio-ventral and anterior views. A, *Panthera leo*. B,  
855 *Panthera onca*. C, *Acynonyx jubatus*. D, *Felis sylvestris*. Cr, cranial; Cd, caudal; L,  
856 left; R, right; V, ventral.

857

858 Figure 4. 3D CT-Scan medial view of the right coxal bone in *Panthera onca*. a, iliac  
859 wing; b, auricular surface dorsal limb; c, auricular surface ventral limb; d; central  
860 eminence; e; dorso-caudal ridge; f, greater sciatic notch.

861

862 Figure 5. Different iliac auricular surfaces outline shapes. A, 3 types defined by Jesse  
863 et al. (2017) in humans (examples on the right surface): a, Type 1 (scone-shaped); b,  
864 Type 2 (auricle-shaped), Type 3 (crescent-shaped). B, 6 different shapes found in  
865 studied felids (examples on the left surface): a, Type 1 (auricle-shaped); b, Type 2  
866 (crescent-shaped); c, Type 3 (spatula-shaped); d, Type 4 (bifoliate-shaped); e, Type  
867 5 (B-shaped); f, Type 6 (Phrygian cap-shaped). Cr, cranial; Cd, caudal; D, dorsal; V,  
868 ventral. Felid species are represented as follow: a, *Panthera onca*; b and c, *Panthera*  
869 *uncial*; d and f *Panthera tigris*; e, *Panthera leo*.

870

871 Figure 6. Examples of the right iliac auricular surface topography in studied species  
872 of Felids. A-B, *Panthera Leo*. C-D, *Panthera pardus*. E-F, *Acynonix jubatus*. G-H,  
873 *Felis sylvestris*. Left column: medio-ventro-dorsal views. Right column: CT-Scan 3D  
874 reconstruction of the same surface, medial view. a, iliac wing; b, auricular surface  
875 dorsal limb; c, auricular surface ventral limb; d; central eminence; e; dorso-caudal  
876 ridge. Purple shades highlight wave-like striations of the auricular surface.

877

878 Figure 7. CT-Scan views showing the inner shape and the outline of the right iliac  
879 auricular surface in *Panthera onca*. Cubes indicate the position of the five views in  
880 the space: Cr, Cranial; D, dorsal; M, medial; V, ventral. A-G: frontal slides. H-N:  
881 transversal slides.

882

883 Figure 8. Views of CT-scan images, 1, longitudinal slide; 2, transversal slide of both  
884 right and left iliac. Comparative shape of the dorso-caudal ridge in small and big cats.  
885 (A) Puma, Caracal, Lynx, and Domestic cat lineages. (B) *Panthera* lineage. The  
886 species are: a, *Acinonyx jubatus*; b, *Leptailurus serval*; c, *Lynx canadensis*; d, *Lynx*  
887 *rufus*; e, *Felis sylvestris*; f, *Panthera leo*; g, *Panthera tigris*; h, *Panthera onca*; i,  
888 *Neofelis nebulosa*; j, *Panthera pardus*; k, *Panthera uncia*. Brackets indicate the right  
889 dorsal limb area. Two shapes of surfaces were determined on the basis of CT-Scan  
890 transversal slides. C, C-shape of the dorsal limb; Cd, Caudal; Cr, Cranial; D, Dorsal;  
891 f, frontal slide of iliac auricular surfaces; L, Left; R, Right; S, S-shape of the dorsal  
892 limb; t, transversal slide of iliac auricular surfaces; V, Ventral.

893

894 Figure 9. PCAs performed on the morphometric data of the iliac auricular surface. A,  
895 C. Right auricular surface. B,D. Left auricular surface. A-B. Plots of the lineages. C-D.  
896 Plots of the ratios. The lineages and ratios are represented by colored dots indicated  
897 in each of the graphs. Ratio 1,  $MPM/PBM \geq 1.9$ ; ratio 2,  $MPM/PBM 1.0 - 1.7$ ; ratio 3,  
898  $MPM/PBM \leq 0.9$ .

899

900 Figure 10. Box plots representing the morphological level of selected landmarks  
901 along (A, B) the outer line (landmarks 2-1-8-7-6-5-4) and (C, D) the inner line  
902 (landmarks 1-9-10-11-5) of the iliac auricular surface. Each line connects dorsal to  
903 ventral landmarks medians. (A, C) species with body mass  $> 14.5$  kg; (B, D) species  
904 with body mass  $< 14.5$  kg.

905

906 Figure 11. Box plots representing the morphological level of selected landmarks  
907 along (A, B) the outer line (landmarks 2-1-8-7-6-5-4) and (C, D) the inner line  
908 (landmarks 1-9-10-11-5) of the iliac auricular surface. Each line connects dorsal to  
909 ventral landmarks medians. (A, C) species with  $MPM/PBM \geq 1$ ; (B, D) species with  
910  $MPM/PBM < 1$ .

911

912 Figure 12. Theoretical shape of the sacro-iliac junction on a pelvis frontal plane in  
913 felids. A, lineages with  $MPM/PBM < 1$ . B, lineages with  $MPM/PBM \geq 1$ . a, iliac wing;  
914 b, sacrum; D, dorsal; L, left; R, right; V, ventral.

915

916 **APPENDIX 1**

917

918 For each iliac auricular surface, we define the plane including landmark 2  
919 (Pt2(x2,y2,z2)), landmark 3 (Pt3(x3,y3,z3)) and landmark 4 (Pt4(x4,y4,z4)).

920

921 We consider Pt3 as the origin of the new coordinate system.

922 Vectors  $\overrightarrow{Pt3Pt2} = (Pt2-Pt3)$  and  $\overrightarrow{Pt3Pt4} = (Pt4-Pt3)$  are calculated as follow:

923

924  $\overrightarrow{Pt3Pt2} (x_{32}, y_{32}, z_{32})$   $x_{32} = x_2 - x_3$

925  $y_{32} = y_2 - y_3$

926  $z_{32} = z_2 - z_3$

927

928  $\overrightarrow{Pt3Pt4} (x_{34}, y_{34}, z_{34})$   $x_{34} = x_4 - x_3$

929  $y_{34} = y_4 - y_3$

930  $z_{34} = z_4 - z_3$

931

932 We calculate the coordinates (X,Y,Z) of a vector  $\vec{V}$  normal to vectors  $\overrightarrow{Pt3Pt2}$  and  
933  $\overrightarrow{Pt3Pt4}$  :

934

935  $X = y_{32} \cdot z_{34} - z_{32} \cdot y_{34}$

936  $Y = z_{32} \cdot x_{34} - x_{32} \cdot z_{34}$

937  $Z = x_{32} \cdot y_{34} - y_{32} \cdot x_{34}$

938

939 In order to find the coordinates (Xn,Yn,Zn) of this normalized vector  $\vec{V}_n$  we first have to  
940 calculate its length (L):

941

942 
$$L = \sqrt{X^2 + Y^2 + Z^2}$$

943

944 The coordinates of  $\vec{V}_n$  orthonormal to the plan are calculated:

945

946  $X_n = X : L$

947  $Y_n = Y : L$

948  $Z_n = Y : L$

949

950 The distance (d) of each point (n,m,p) from the plane including Pt2, Pt3 and Pt4 is  
951 given by the equation:

952

$$953 \quad d = (n - x_3) \cdot X_n + (m - y_3) \cdot Y_n + (p - z_3) \cdot Z_n$$

954

955 To compare the distance of each point to the plane within various sized auricular  
956 surfaces, the relative distance of each point to the plane was given in percentage  
957 ( $d\%$ ) of the distance of landmark 1 ( $d_1$ ) to the plane. Landmark 1 is selected because  
958 it is the most dorsal point of each articulation regardless their size and shape. For  
959 each landmark,  $d\%$  is given by:

960

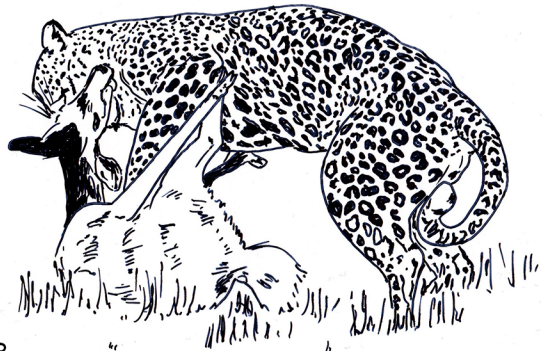
$$961 \quad d\% = (d : d_1) \cdot 100$$

962

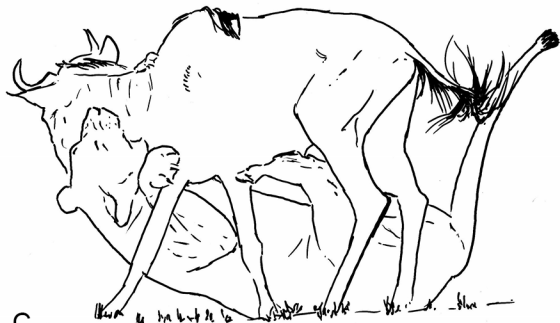
963  $d\%$  measures the difference in level of each landmark towards the plane including  
964 landmarks 2, 3 and 4. According to our calculation  $d\%=0$  for landmarks 2, 3 and 4  
965 and  $d\%=100$  for landmark 1.



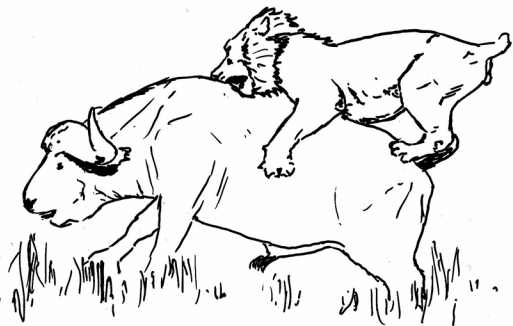
A



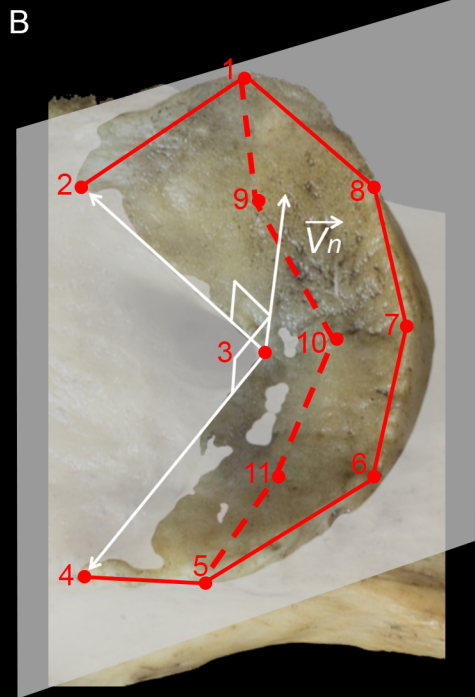
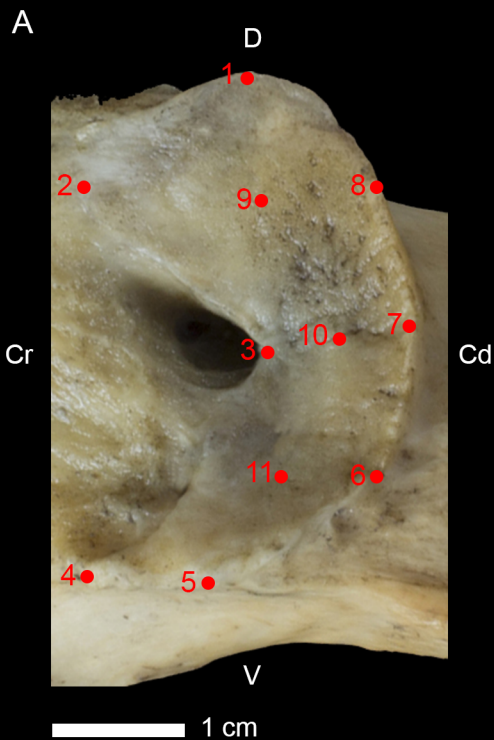
B



C



D



Dorsal

R



Cranio-ventral

L

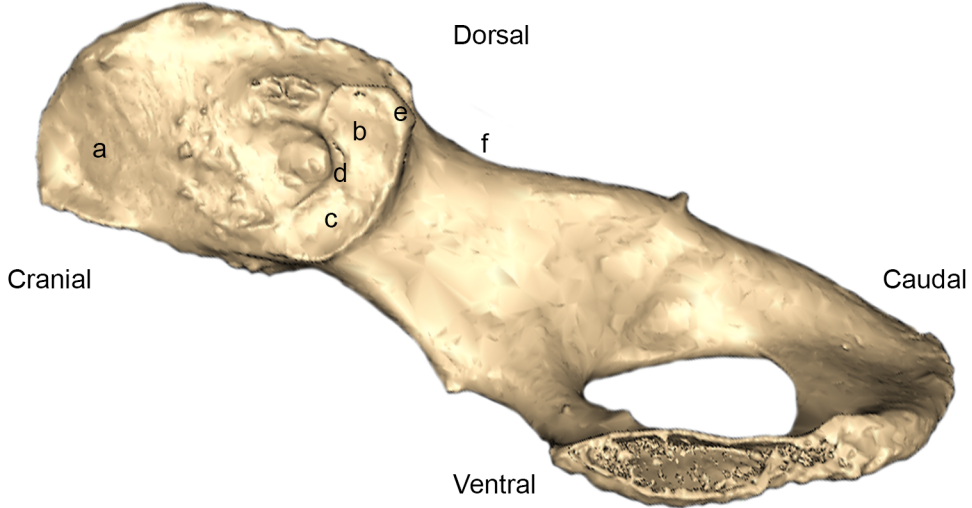


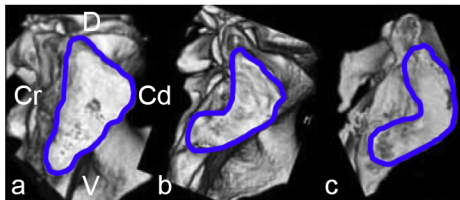
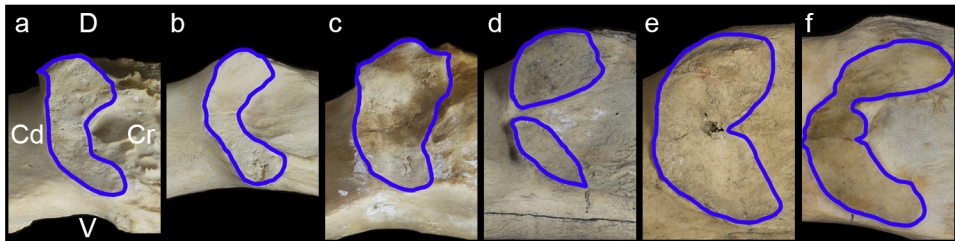
Anterior

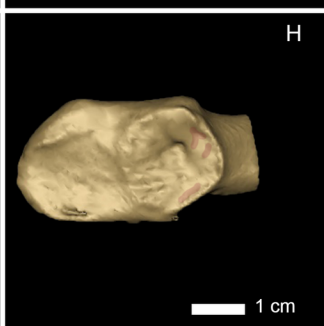
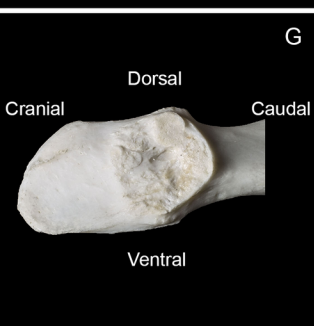
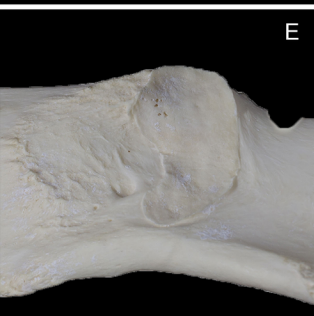
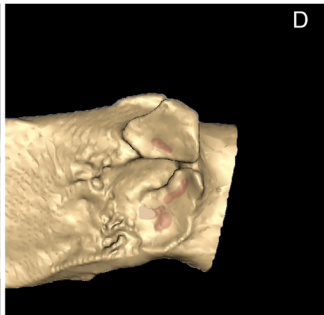
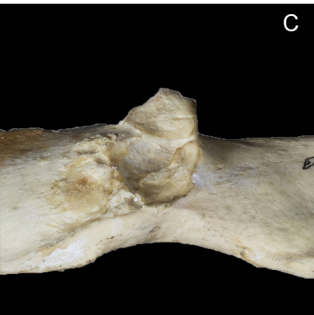
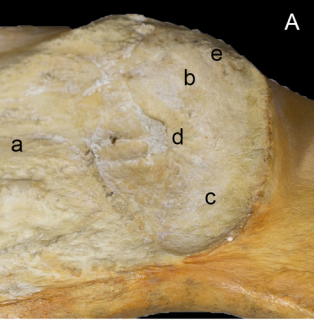
R

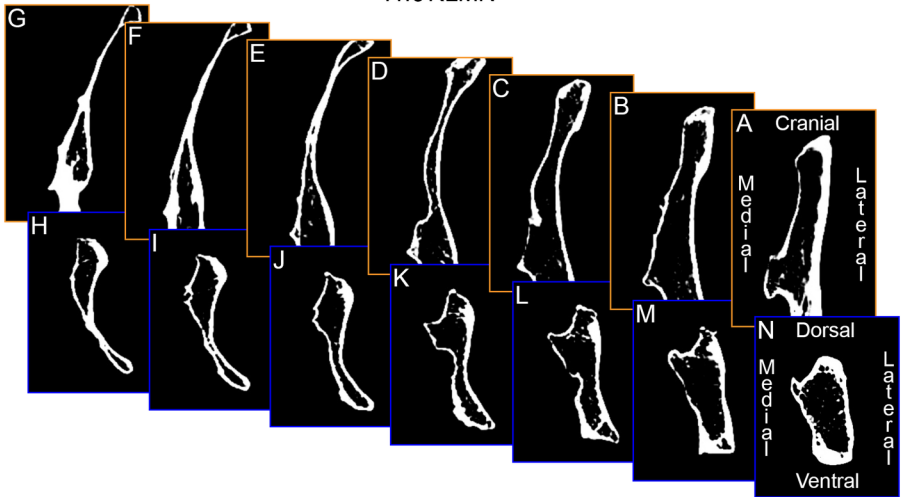
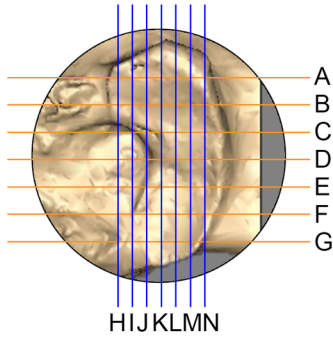
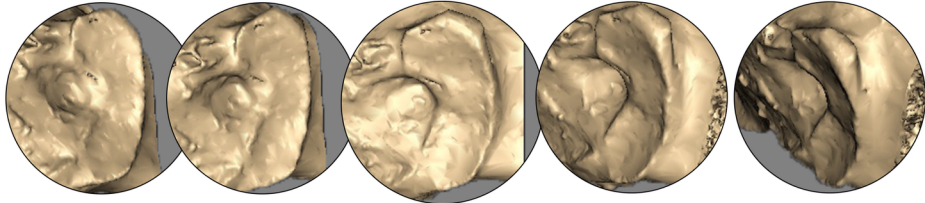
L

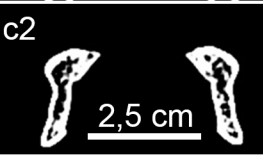
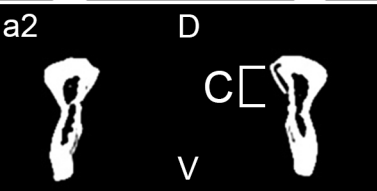
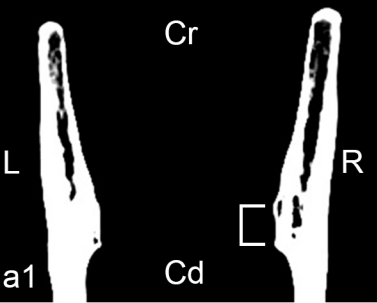


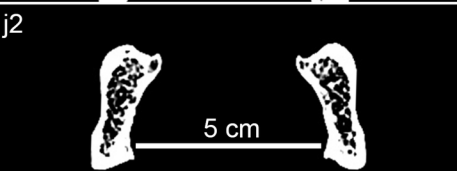
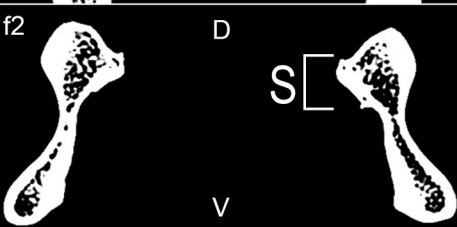
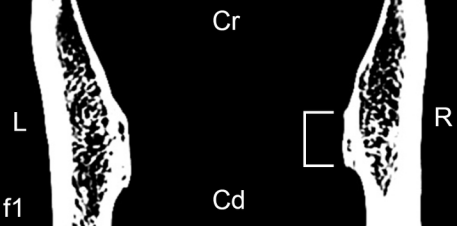


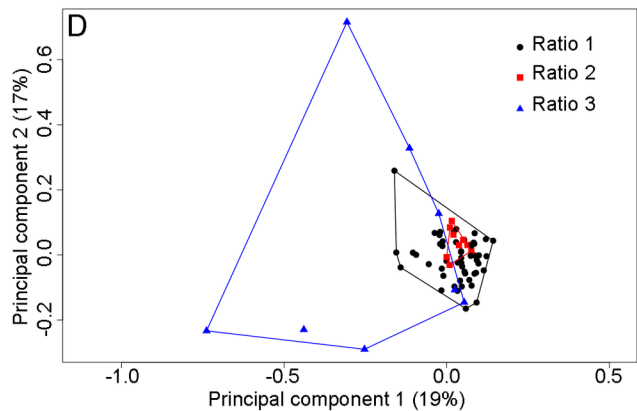
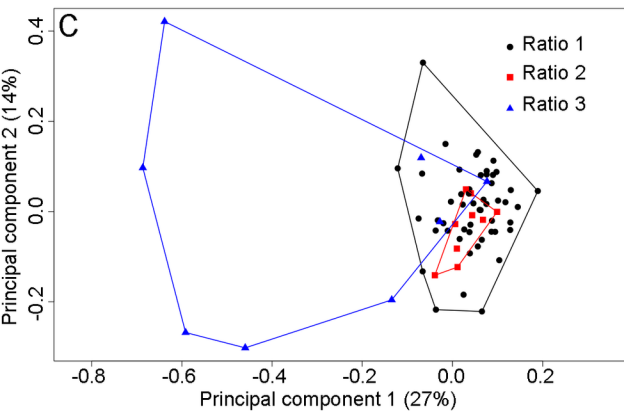
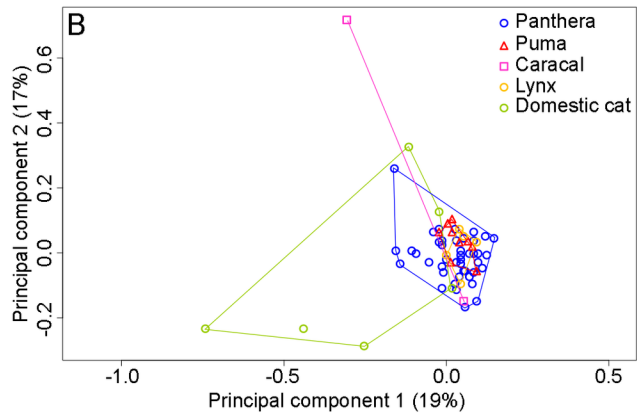
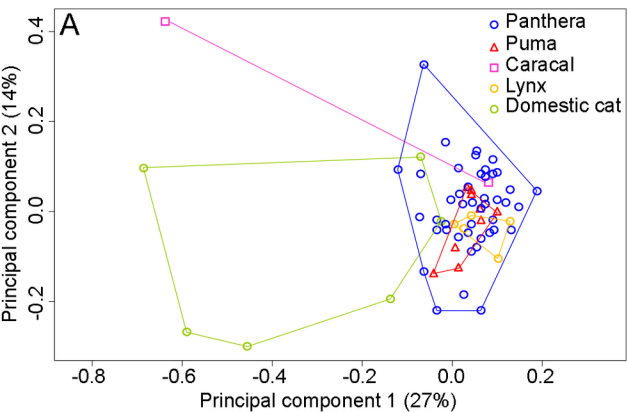
**A****B****1 cm**

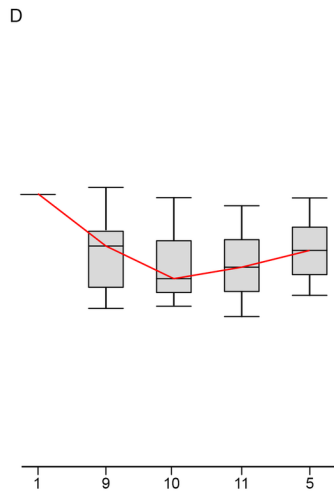
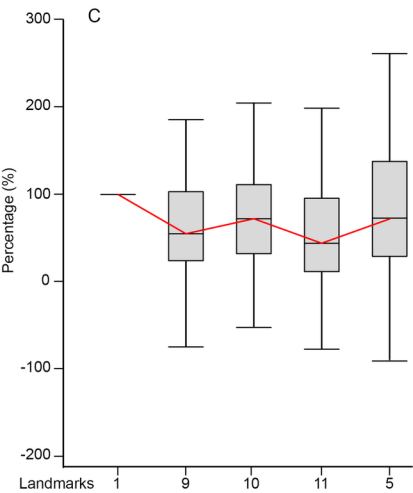
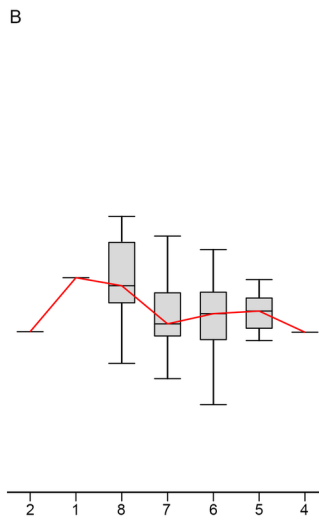
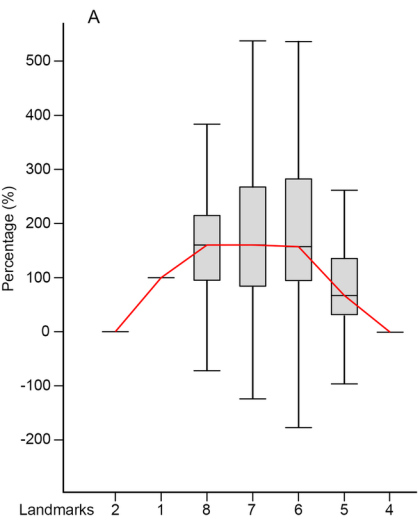


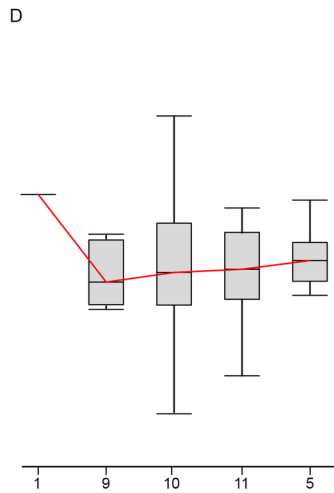
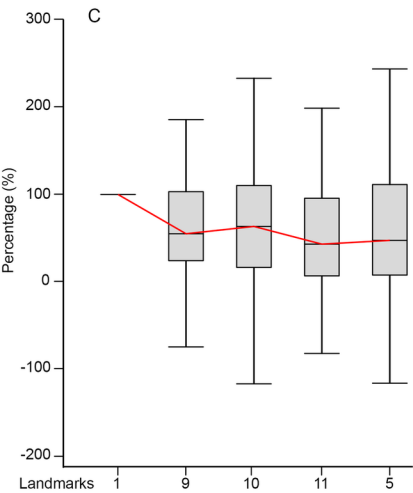
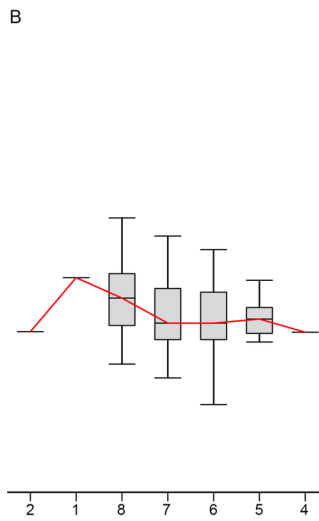
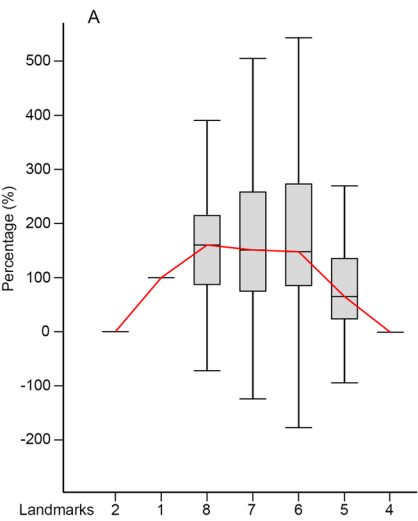












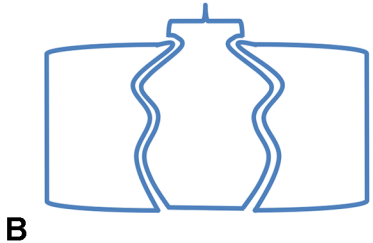
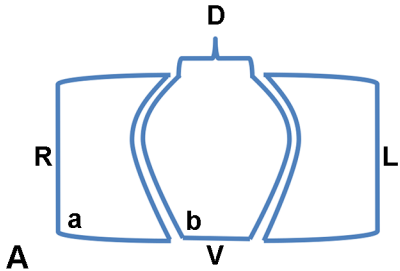


Table 1. Felid species used in this study.

(1) Sicuro and Oliveira (2011), (2) Meachen-Samuels and Van Valkenburgh (2009b), (3) Samuels et al. (2013), (T)\* Terrestrial locomotor class following Meachen-Samuels and Van Valkenburgh (2009b), (4) Sunquist and Sunquist (2017), (5) Kitchener et al. (2010), (6) Schaller and Vasconcellos (1978). MPM/PBM ratio classes are defined as follow: ratio 1,  $\geq 1.9$ ; ratio 2, 1.0 - 1.7; ratio 3,  $\leq 0.9$ . Ratios between brackets are the values calculated by Sicuro and Oliveira (2011), MPM: Maximum average prey mass, PBM: Average predator body mass.

Species	Lineage	Number of specimens	Average body mass (kg) <sup>(1)</sup>	Body mass range (kg) <sup>(2)</sup>	Locomotor classes <sup>(3)</sup>	MPM/PBM <sup>(1)</sup> classes	Hunting strategy <sup>(4)</sup>	Bite <sup>(5)(6)</sup>
<i>Acinonyx jubatus</i>	Puma	7	53.5	40-65	Cursorial (T)*	2 (1.0)	Solitary	Suffocation
<i>Felis silvestris</i>	Domestic cat	6	5.5	3-6	Scansorial	3 (0.7)	Solitary	Spine
<i>Leptailurus serval</i>	Caracal	2	13.4	8-18	Terrestrial	3 (0.4)	Solitary	Spine
<i>Lynx canadensis</i>	Lynx	2	11.2	5-17	Terrestrial	2 (1.2)	Solitary	Spine
<i>Lynx rufus</i>	Lynx	3	11.2	4-16	Scansorial	1 (2.4)	Solitary	Spine
<i>Neofelis nebulosa</i>	Panthera	2	19.5	11-25	Arboreal	1 (2.7)	Solitary	Suffocation
<i>Panthera leo</i>	Panthera	14	185.0	110-250	Terrestrial	1 (2.3)	Pack	Suffocation
<i>Panthera onca</i>	Panthera	5	105.7	36-120	Scansorial	1 (2.0)	Solitary	Back of skull
<i>Panthera pardus</i>	Panthera	12	59.0	28-65	Scansorial	1 (2.0)	Solitary	Suffocation
<i>Panthera tigris</i>	Panthera	11	185.5	75-325	Terrestrial	1 (2.7)	Solitary	Suffocation
<i>Panthera uncia</i>	Panthera	2	50.0	22-52	Scansorial	1 (1.9)	Solitary	Suffocation
<i>Puma concolor</i>	Puma	2	67.5	23-80	Scansorial	2 (1.7)	Solitary	Suffocation

**Table 2.** Landmarks used in analysis (and see Fig. 4). Landmark 9 is the highest or the deepest point of the dorsal limb of the articular surface whether it is convex or concave. Landmark 11 is the highest or the deepest point of the ventral limb of the articular surface whether it is convex or concave.

---

Number	Definition of landmark
1	Dorsalmost point of the articular surface
2	Anteriormost point of the dorsal limb of the articular surface
3	Posteriormost point of the cranial border
4	Anteriormost point of the ventral limb of the articular surface
5	Ventralmost point of the articular surface
6	Midpoint between 5 and 7 on the caudal border line
7	Posteriormost point of the caudal border
8	Midpoint between 7 and 1 on the caudal border line
9	Deepest or highest point of the dorsal limb of the articular surface
10	Midpoint between 3 and 7
11	Deepest or highest point of the ventral limb of the articular surface

---

Table 3. Estimated means and groups calculated using a Tukey's test on the two first axes obtained from the PCAs based on landmarks determined on the iliac articular surface. A. Comparison between the studied felid lineages. B. Comparison between the three MPM/PBM ratio classes determined from the literature (Table 1). Comparison between bite types.

A								
Lineages	Right				Left			
	PC1		PC2		PC1		PC2	
	Estimated mean	Group						
Caracal	-0.281	B	0.244	A	-0.127	AB	0.285	A
Domestic cat	-0.328	B	-0.095	B	-0.258	B	-0.068	B
Lynx	0.062	A	-0.042	B	0.042	A	0.011	AB
Panthera	0.041	A	0.011	B	0.028	A	-0.011	B
Puma	0.035	A	-0.026	B	0.033	A	0.033	AB

B								
MPM/PBM class	Right				Left			
	PC1		PC2		PC1		PC2	
	Estimated mean	Group						
1	0.044	A	0.007	A	0.030	A	-0.010	A
2	0.033	A	-0.024	A	0.032	A	0.031	A
3	-0.316	B	-0.011	A	-0.225	B	0.020	A

C				
Bite	Right			
	PC1		PC2	
	Estimated mean	Group	Estimated mean	Group
Suffocation	0.040	A	-0.001	A
Spine	-0.316	B	-0.011	A
Skull	0.061	A	0.024	A

Table 4. Mann-Whitney tests of ecological factors effect on landmarks difference in level. The significant level was selected at p-value < 0.05.

Factors	Tests	Landmarks						
		5	6	7	8	9	10	11
Body mass class	U	1514	1870	1746	1377	1256	1442	1298
	p-value	0,003	< 0.0001	< 0.0001	0,007	0,098	< 0.0001	0,01
MPM/PBM 1-2 vs 3	U	956	1128	1105	938	872	829	728
	p-value	0,007	< 0.0001	< 0.0001	0,004	0,02	0,038	0,139